

Mobile harbor: structural dynamic response of RORI crane to wave-induced rolling excitation

Jin-Rae Cho^{*1,2}, Ki-Chul Han¹, Soon-Wook Hwang¹, Choon-Soo Cho¹ and O-Kaung Lim¹

¹*School of Mechanical Engineering, Pusan National University, Busan 609-735, Korea*

²*Research & Development Institute of Midas IT, Gyeonggi-Do 463-400, Korea*

(Received April 18, 2012, Revised August 8, 2012, Accepted August 9, 2012)

Abstract. A new concept sea-floating port called mobile harbor has been introduced, in order to resolve the limitation of current above-ground port facilities against the continuous growth of worldwide marine transportation. One of important subjects in the design of a mobile harbor is to secure the dynamic stability against wave-induced excitation, because a relatively large-scale heavy crane system installed at the top of mobile harbor should load/unload containers at sea under the sea state up to level 3. In this context, this paper addresses a two-step sequential analytical-numerical method for analyzing the structural dynamic response of the mobile harbor crane system to the wave-induced rolling excitation. The rigid ship motion of mobile harbor by wave is analytically solved, and the flexible dynamic response of the crane system by the rigid ship motion is analyzed by the finite element method. The hydrodynamic effect between sea water and mobile harbor is reflected by means of the added moment of inertia.

Keywords: mobile harbor; roll-out roll-in (RORI) crane; wave-induced excitation; rigid ship roll motion; structural dynamic response; finite element analysis

1. Introduction

Carriage amount of goods by ship is continuously increasing in proportion to the worldwide intensive trade activities, which inevitably requires container carriers with larger carrying capacity. However, being large scale of container carrier gives rise to severe problems in current above-ground port facilities, such as the difficulty in coming to ports and the considerable delay in loading and unloading operations. Mobile harbor is meant by a new concept floating-type port introduced to resolve these inherent problems which current above-ground port facilities face. This new concept port is able to unload and load containers on the sea, by sailing between container carriers on the coast and the conventional above-ground ports. It can be imagined as a specially designed carrier equipped with crane system.

To make this concept feasible, mobile harbor should fulfill several requirements; the compact size and lightweight, the sufficient structural strength, and the dynamic stability at both working and sailing modes. And these requirements are greatly influenced by the crane system installed on the

*Corresponding author, Vice Director, E-mail: jrcho@pusan.ac.kr

mobile harbor, because the crane system is not only installed at the top but it has the outreach length much larger than the mobile harbor dimension. For this reason, a crane system which is able to be folded at sailing and unfolded at working is preferable, and a roll-out roll-in (RORI) type crane system (Lim *et al.* 2010) is introduced in this paper. A RORI crane system is composed of a fixed main and two extendable horizontal booms, and a rotatable vertical (apex) boom, where two extendable booms are able to slide in and out through the fixed main boom. A mobile harbor equipped with RORI crane system under consideration in the current study is designed to handle 5,000TEU paramax container carriers, such that it can load/unload 30 twenty five-ton containers per hour with a maximum carrying capacity of 250TEU at the sea state up to level 3.

The goal of this study is to evaluate the transient structural dynamic response of the mobile harbor equipped with RORI crane system subject to the wave excitation up to the sea state 3, by neglecting wind load. Roll motion among six degrees of freedom of mobile harbor is considered because this excitation component is most critical (Senjanovic *et al.* 1997) to the mobile harbor equipped with RORI crane with horizontal booms which outreach in the direction to perpendicular to the ship heading axis. The rigid roll motion of mobile harbor by sinusoidal beam wave at sea state 3 is analytically obtained according to the linear wave theory (Biran 2003, Lee 2003), by assuming that the mobile harbor is rigid and the wave is incompressible, invicid and irrotational. And, the transient dynamic response of the flexible mobile harbor subject to the rigid roll motion is analyzed by the finite element analysis. The hydrodynamic interaction between the mobile harbor and the wave is taken into consideration by means of the added mass (Rajasankar *et al.* 1993, Cho and Song 2001, Cho *et al.* 2001). Through the numerical experiments, the dynamic responses of RORI crane system when the mobile harbor is empty or full loaded are examined. As well, the dynamic suppression effect of counter and inflated rubber fender are investigated.

2. Problem description

2.1 Mobile harbor with RORI crane system

Two-dimensional section view of mobile harbor equipped with RORI crane system which is fully unfolded during unloading and loading of containers is represented in Fig. 1(a), where 1st and 2nd sliding booms supported by cables and foldable elastic bar are able to slide in and out the main fixed boom. And, the vertical apex boom is able to rotate on the hinge located at the right end of the main boom. The configuration of the mobile harbor completely folded in sailing mode is represented in Fig. 1(b). In order for the dynamic stability of the mobile harbor, a counter weight with the total mass m_{cw} and two inflated rubber fenders are attached to the left end of the main boom and to the right side of the mobile harbor, respectively. The overall geometric dimensions of the mobile harbor are as follows: $B = 30$ m, $H_m = 10.5$ m, $H_c = 35$ m, $B_{cw} = 10$ m and the ship length $L = 70$ m, and the height H_a and the outreached total length of RORI crane system are 30, 8 and 40 m, respectively.

The weight of the mobile harbor when containers are not loaded is 3,547 ton, including the RORI crane system (360 ton), while the total weight of the mobile harbor reaches 7,650 ton when 250 units of containers are fully loaded. The mobile harbor is designed to sail on the coastal water with the maximum depth 5 m with the average sailing speed 8 knot, at the sea state up to the level 3. Containers are unloaded to the mobile harbor and loaded to the container carrier by trolley which is

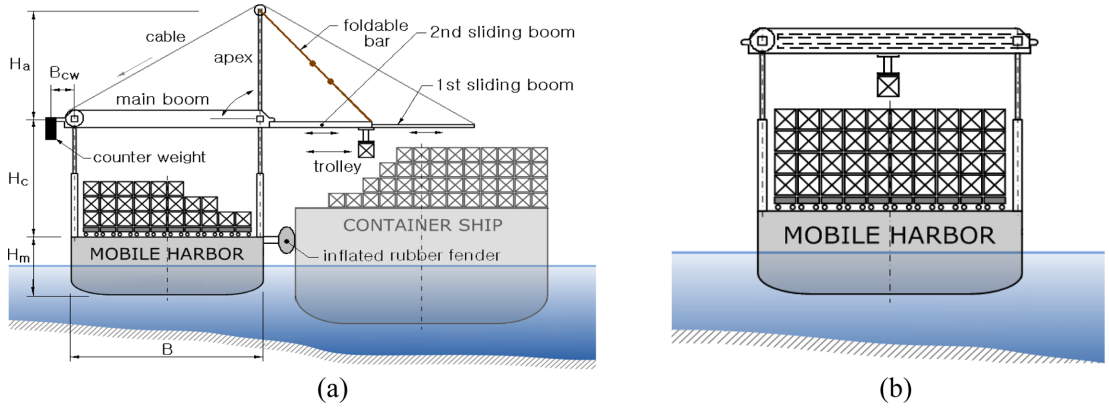


Fig. 1 Configuration of mobile harbor: (a) working mode, (b) sailing mode

designed to move along the sliding booms, and the most cautious job in the loading and unloading operations is the precise positioning of the trolley to pick the target container and to put the container at the target position. Even though the trolley motion is controlled by the electric control system, the dynamic structural vibration at the tip of 1st sliding boom under the sea state 3 is highly desirable to be minimized. For this reason, several devices such as counter-balancing mass, anti-vibration damper, floating fender, and bubble effect hydraulic system (Godeauy and Grist 2006) are needed to be attached to either the mobile harbor body or to the crane system. However, the most and first step before designing these dynamic stabilization devices is to analyze the inherent structural dynamic characteristics of the mobile harbor crane system itself subject to the wave motion at sea state 3.

2.2 Wave-induced rigid roll motion of mobile harbor

Referring to Fig. 2(a), the rigid ship motion $\mathbf{R} \in \mathcal{R}^3$ is decomposed into the rigid translation $\mathbf{s} \in \mathcal{R}^3$ and the rigid rotation $\mathbf{\Omega} \in \mathcal{R}^3$ such that

$$\mathbf{R} = \mathbf{s} \oplus \mathbf{r} \times \mathbf{\Omega} \quad (1)$$

$$\mathbf{s} = \eta_1 \mathbf{i} + \eta_2 \mathbf{j} + \eta_3 \mathbf{k}, \quad \mathbf{\Omega} = \eta_4 \mathbf{i} + \eta_5 \mathbf{j} + \eta_6 \mathbf{k} \quad (2)$$

In which η_1, η_2 and η_3 denote surge, sway and heave motions, while η_4, η_5 and η_6 indicate roll, pitch and yaw motions, respectively.

Introducing the (6×6) wave and viscous damping matrices \mathbf{B} and \mathbf{b} , the added mass (or, moment of inertia) matrix \mathbf{A} and the restoring stiffness matrix \mathbf{C} , the generalized coupled rigid ship motions are expressed by Biran (2003)

$$(\mathbf{M} + \mathbf{A})\ddot{\boldsymbol{\eta}} + (\mathbf{B} + \mathbf{b} \delta_{4j})\dot{\boldsymbol{\eta}} + \mathbf{C} \boldsymbol{\eta} = \text{Re}(\mathbf{F} e^{i\omega_E t}) \quad (3)$$

In which, \mathbf{M} and $\text{Re}(\mathbf{F} e^{-i\omega_E t}) F_i^w$ denote the ship mass (or, moment of inertia) matrix and the vector of sinusoidal exciting force and moment. In addition, the encounter frequency ω_E is calculated by

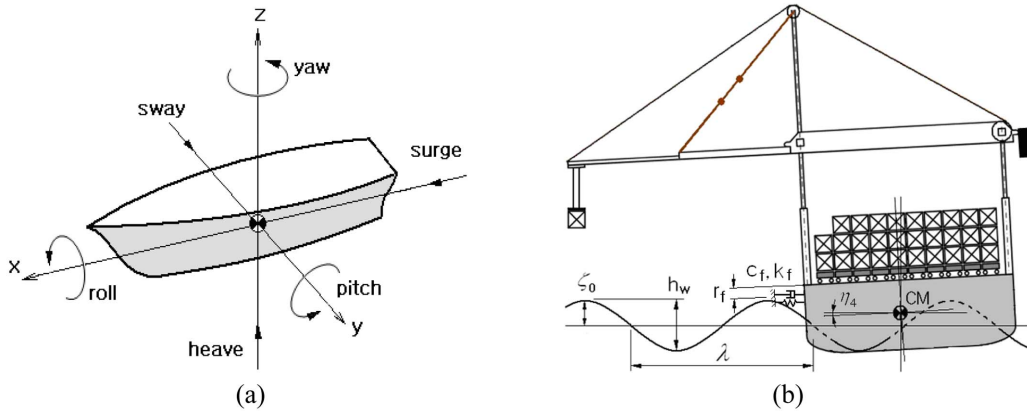


Fig. 2 Representation: (a) rigid ship motion with 6-DOFs, (b) rigid roll motion of mobile harbor by sinusoidal beam wave

$$\omega_E = \omega_w - \frac{\omega_w^2}{g} u \cos \mu \tag{4}$$

with the wave frequency ω_w , the ship velocity u and the encounter angle μ . The water viscous damping is known to be remarkable in roll motion, when compared to the wave damping, but its effect in roll motion disappears when the flow is assumed to be inviscid.

According to the Pierson-Moskowitz sea spectrum (1964), the wave length λ and the wave height h_w at sea state 3 are known as $\lambda = 13.8\sim 15.8$ m and $h_w = 1.05\sim 1.2$ m. The wave height which is not significant but regular is taken because containers should be carefully and safely delivered between the paramax container carrier and the ground harbor. The outreach of RORI crane system in the lateral direction (i.e., in the y -direction) makes the mobile harbor sensitive to the roll excitation, as shown in Fig. 2(b), where, c_f and k_f denote the resulting damping coefficient and the spring constant of the inflated rubber fender. Furthermore, the wave length is small compared to the width of mobile harbor so that the heave motion is not significant. So, for the current study, we consider only the rigid roll motion of the mobile harbor by a sinusoidal beam wave with the encounter angle $\mu = 90^\circ$ or 270° .

Neglecting the coupling with the pitch motion and using the relation of $\omega_E = \omega_w$, the uncoupled rigid roll motion is expressed by

$$(I_{44} + J_{44}) \ddot{\eta}_4 + B_{44} \dot{\eta}_4 + C_{44} \eta_4 = Re(F_4 e^{i\omega_w t}) \tag{5}$$

with the roll moment of inertia I_{44} of ship and the added roll moment of inertia J_{44} . And, the restoring stiffness in which both the buoyancy stiffness and the fender stiffness k_f are combined is calculated by $C_{44} = W \cdot \overline{GZ}$ and the wave-induced roll moment in the RHS of Eq. (5) is expressed by

$$Re(F_4 e^{i\omega_w t}) = W \cdot \overline{GZ} \cdot \gamma \cdot \Theta \cos \omega_w t \tag{6}$$

with the total ship weight W , the righting arm \overline{GZ} , the effective wave slope coefficient γ and the peak wave slope: $\Theta = 2\pi\zeta_0/\lambda$ (Biran 2003, Lee 2003).

Substituting these relations into Eq. (5) and dividing the resulting equation by $(I_{44} + J_{44})$ ends up with a second-order ODE given by

$$\ddot{\eta}_4 + 2n\dot{\eta}_4 + \omega_{n4}^2 \eta_4 = \omega_{n4}^2 \gamma \frac{2\pi\zeta_0}{\lambda} \cos \omega_w t \quad (7)$$

to solve the rigid roll response $\eta(t)$ of ship. Here, $n = (W \cdot \overline{GZ}) / 2(I_{44} + J_{44})$ is a linear damping coefficient including the fender damping coefficient c_f and $\omega_{n4} = \sqrt{(W \cdot \overline{GZ}) / (I_{44} + J_{44})}$ is the ship natural angular frequency, from which both are in relation of $n = \omega_n^2 / 2$. Meanwhile, the added moment of inertia J_{44} is in function of the ship geometry, the ship motion, the water depth and the natural frequency (Biran 2003, Lee 2003, Cho and Song 2001), but empirically it has been known that $(I_{44} + J_{44}) \cong m(0.4B)^2$ (Lee 2003).

3. Structural dynamic response of the flexible mobile harbor

The absolute dynamic displacement $\mathbf{u}(\mathbf{x};t)$ at a point \mathbf{x} within the flexible mobile harbor under the rigid roll motion centered at the mass center of mobile harbor is expressed by

$$\mathbf{z}(\mathbf{x};t) = \mathbf{r}(\mathbf{x}) \times \eta_4(t) \mathbf{i} + \mathbf{u}(\mathbf{x};t) \quad (8)$$

where $\mathbf{r}(\mathbf{x})$ denotes the position vector to the point x from the mass center. Then, the damped dynamic displacement of the flexible mobile harbor is governed by

$$\nabla \cdot \boldsymbol{\sigma}(\mathbf{u}) - c\mathbf{u} + \mathbf{f} = \rho \frac{\partial^2}{\partial t^2} \{ \mathbf{z} - \mathbf{r}(\mathbf{x}) \times \eta_4(t) \mathbf{i} \} \quad (9)$$

with the Cauchy stress tensor $\boldsymbol{\sigma}(\mathbf{u})$, the structural damping coefficient c , the body force \mathbf{f} , and the mass density ρ .

Introducing N iso-parametric basis functions $\{ \phi_j(\mathbf{x}) \}$ into the Galerkin approximation of Eq. (9) leads to

$$([\mathbf{M}] + [\mathbf{M}_{add}]) \ddot{\bar{\mathbf{u}}} + [\mathbf{C}] \dot{\bar{\mathbf{u}}} + [\mathbf{K}] \bar{\mathbf{u}} = -([\mathbf{M}] + [\mathbf{M}_{add}]) (\mathbf{r} \times \ddot{\eta}_4 \mathbf{i}) \quad (10)$$

Moreover, in the space of eigen modes, the damped dynamic displacement can be expressed as a linear combination of natural modes $\Phi_j(\mathbf{x})$ and the modal participation coefficients $q_j(t)$

$$\bar{\mathbf{u}}(\mathbf{x};t) = \sum_{j=1}^N q_j(t) \cdot \Phi_j(\mathbf{x}) \quad (11)$$

By letting $([\mathbf{M}] + [\mathbf{M}_{add}])$ be $[\tilde{\mathbf{M}}]$, Eq. (10) can be rewritten as

$$\sum_{j=1}^N \{ [\tilde{\mathbf{M}}] \Phi_j \ddot{q}_j + [\mathbf{C}] \Phi_j \dot{q}_j + [\mathbf{K}] \Phi_j q_j \} = \mathbf{P}_{eff} \quad (12)$$

with the effective dynamic force defined by

$$\mathbf{P}_{eff} = -[\tilde{\mathbf{M}}] (\ddot{\eta}_3 \mathbf{k} + \mathbf{r}(\mathbf{k}) \times \ddot{\eta}_4 \mathbf{i}) \quad (13)$$

Multiplying Φ_k to Eq. (12) and using the M-orthonormality of the eigen modes, one can easily obtain the N decoupled second-order ODEs given by

$$\ddot{q}_k(t) + 2\zeta_k\omega_k\dot{q}_k(t) + \omega_k^2q_k(t) = Q_k \quad (14)$$

to compute the participation coefficients. In which, ζ_k and $Q_k(=\Phi_k\mathbf{P}_{eff})$ denote the damping ratio and the normalized force at the k -th natural mode of the flexible mobile harbor, respectively.

4. Numerical results

A series of two sequential numerical analyses are carried out to solve the flexible structural dynamic response of the mobile harbor. First, a semi-analytical-numerical analysis is performed to solve Eq. (7) for the rigid roll motion of the mobile harbor subject to the sinusoidal beam wave at sea state 3, for which the natural frequency ω_{n4} of the rigid mobile harbor is obtained by the finite element analysis. Next, the dynamic displacement of the flexible mobile harbor is solved by 2-D explicit finite element method. Referring to Fig. 1(a), the geometric dimensions of 3-D mobile harbor are as follows: the length $L = 70$ m, the width $B = 30$ m, the outreach of extendable booms $B_{ext} = 40$ m, the working area height $H_c = 35$ m the ship height $H_m = 10.5$ m, respectively. The total mass and the attachment distance of counter weight are set as follows: $m_{cw} = 100$ ton and $B_{cw} = 10$ m, while the resulting spring constant and damping coefficient and the attachment location of the inflated rubber fenders are set by $k_f = 25.5$ kgf/m, $c_f = 36.4$ kgf·sec/m and $r_f = 2.1$ m based upon the the experimental results by Kumho Tire Co. in Korea. Meanwhile, the wave length, the wave frequency and the wave height are set as follows: $\lambda = 24.98$ m, $\omega_w = 1.57$ rad/sec and $\zeta_0 = 0.65$ m.

4.1 Rigid roll motion of mobile harbor

Fig. 3 shows a 2-D finite element model of the mobile harbor which is dimensionally reduced in the ship length direction for which the ship body and containers are modeled as rigid bodies. The horizontal and vertical booms and the foldable bar are modeled with beam elements, while main cables and trolley cables and a container are modeled by means of follower loads and a mass element, respectively. The material properties of booms and foldable bar are as follows: the mass density ρ of $7,850$ kg/m³, Young's modulus E of 200 GPa and Poisson's ratio ν of 0.3 . The buoyancy force of sea water is modeled as an elastic foundation composed of N linear springs with the spring constant $k_s = W/N$. The added moment of inertia J_{44} is imposed in the manner of adjusting the mass densities of the mobile harbor components in the same light such that the relation of $(J_{44} + J_{44}) \cong m(0.4B)^2$ is satisfied approximately.

Five simulation cases are considered: full loaded and empty cases without dynamic stabilizer and full case with counter weight, full case with inflated rubber fenders, and full case with counter weight and inflated rubber fenders, respectively. We first carried out the finite element analysis to compute natural frequencies ω_{n4} of the rigid mobile harbor, for which booms, bar and cables are modeled as rigid. Regarding the essential boundary condition, only the rotational degree of freedom of the mass center is set free.

Rigid roll natural frequencies obtained by finite element analysis for five model cases are

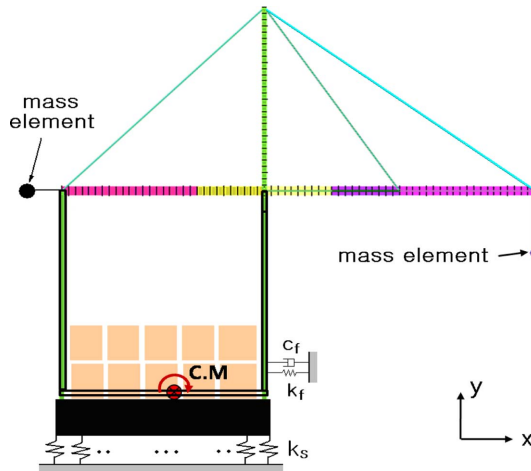


Fig. 3 Finite element model of mobile harbor with RORI crane system

Table 1 Natural frequencies and maximum roll angles of the rigid mobile harbor

Cases	Natural frequency (rad/sec)	Maximum roll angle (rad)	
		Counter-clockwise	Clockwise
Empty	0.9328	0.0693	0.0783
Full loaded	0.7597	0.0443	0.0589
Full with CW	0.7299	0.0416	0.0557
Full with fenders	0.7601	0.0290	0.0330
Full with CW and fenders	0.7312	0.0260	0.0295

compared in Table 1. The empty case exhibits the highest natural frequency while the full loaded case with counter weight does the lowest frequency. On the other hand, the attachment of fenders increases the rigid roll natural frequency of the rigid mobile harbor. It is consistent well with the fact that the increase of mass makes the natural frequency smaller while the increase of damping does the natural frequency larger.

The rigid roll natural frequencies obtained by the finite element analysis with the rigid mobile harbor model were plugged into Eq. (7) to analytically solve the rigid roll response of the rigid mobile harbor on the mass center. Fig. 4(a) compares the roll responses between the empty and full loaded cases, where the significant reduction in the roll amplitude from the empty case to the full loaded case is clearly observed. According to the detailed maximum roll angles given in Table 1, the relative reduction in the maximum roll angle reaches 24.8~36.1%. The effects of counter weight and rubber fender on the rigid roll response of the full loaded mobile harbor are presented in Fig. 4(b), where both counter weight and rubber fender suppress the rigid roll motion of mobile harbor. The effect of counter weight is not remarkable but rubber fender significantly suppresses the rigid roll response. According to the detailed numerical values given in Table 1, the relative reductions of the maximum roll angle from the full loaded case are turned out to be 6.1% by counter weight, 43.5% by rubber fender and 49.9% by the combined use of counter weight and rubber fender, respectively.

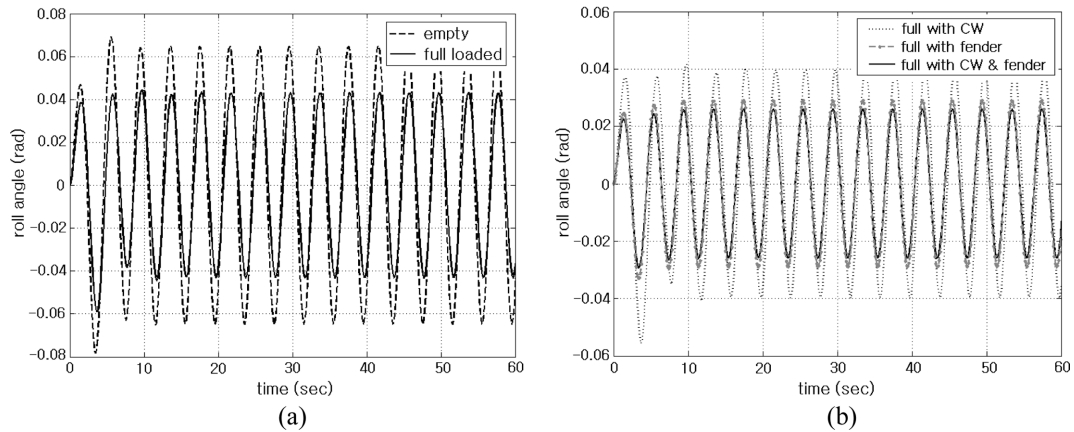


Fig. 4 Rigid roll responses of the mobile harbor: (a) without stabilizer, (b) full loaded with stabilizer

4.2 Structural dynamic response of flexible mobile harbor

As a next step, the flexible dynamic response of RORI crane system subject to the rigid roll motion of mobile harbor is analyzed. Transient dynamic analysis is carried out with the finite element model shown in Fig. 3 in which all the structural components except for the mobile harbor frame and containers are considered flexible. The rigid roll motion solved at the previous step is applied to the mass center of mobile harbor, as an external excitation. Among the dynamic displacements of crane components, the main observation focuses on the dynamic displacement at the tip of first sliding boom because it strongly influences the position controllability in taking down and picking containers during loading and unloading operations. The flexible finite element model is constructed with the total element number of 125, and the time duration of observation T and the time step size Δt are set by 180 and 0.1 sec, respectively.

Time histories of the horizontal and vertical boom tip displacements for full loaded and empty cases are compared in Figs. 5 and 6 respectively, where those of the rigid crane system are included for the comparison purpose. The vertical dynamic displacements are shown to be much larger than the horizontal ones in both cases, but the full case produces the horizontal and vertical dynamic displacements smaller than the empty case. The detailed peak dynamic displacements in both cases are recorded in Table 2, where the peak vertical displacement is larger by 98.4~124.9% than the peak horizontal one while the full loaded case produces the peak displacements smaller by 14.2~24.3% than the empty case. Meanwhile, the flexible crane system produces the dynamic displacements slightly larger than the rigid crane system, in both cases and in both displacement components. In Table 3, the increases of the peak dynamic displacements of the flexible crane system with respect to the rigid crane system are recorder in details. The absolute differences are shown to be smaller in the full loaded case, but it is owing to the difference in the dynamic displacement magnitudes between the full loaded and empty cases. The relative differences with respect to the peak dynamic displacements in both cases are 8.75~9.13% in the horizontal displacement and 10.81~11.95% in the vertical displacement, respectively. It implies that the effect of the crane flexibility on the structural dynamic response of the crane system is not remarkably influenced by whether containers are fully loaded or not.

Time histories of the horizontal and vertical dynamic displacements at the boom tip of the full

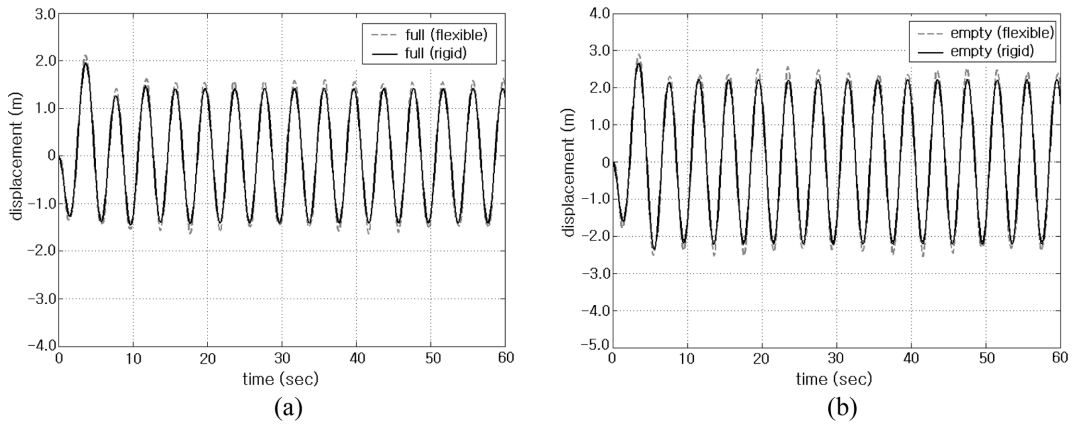


Fig. 5 Time histories of the horizontal boom tip displacement without stabilizer: (a) full, (b) empty

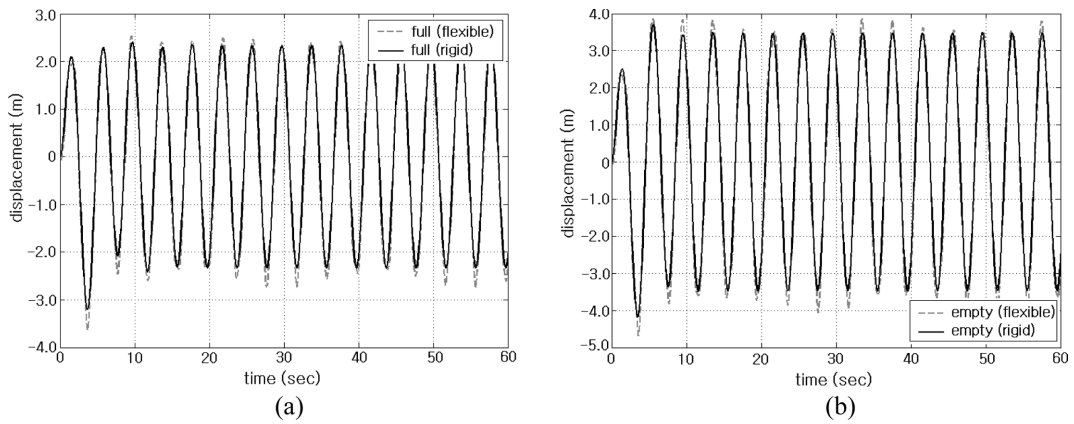


Fig. 6 Time histories of the vertical boom tip displacement without stabilizer: (a) full, (b) empty

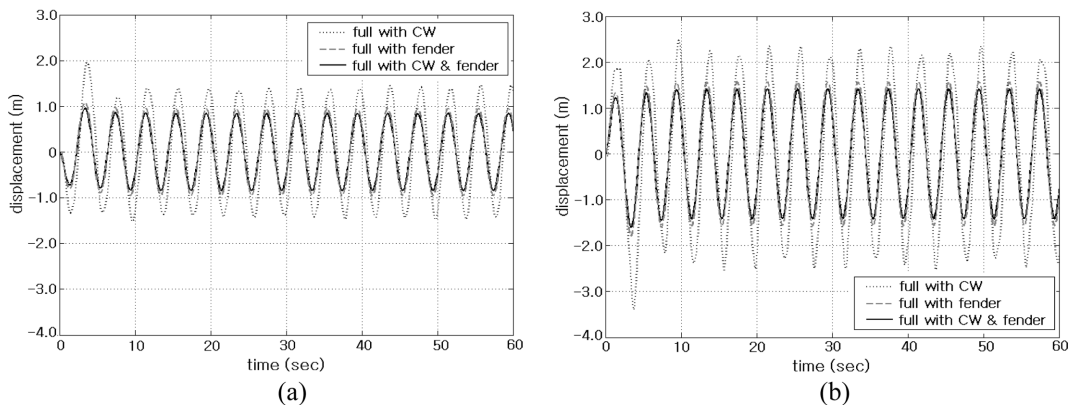


Fig. 7 Time histories of the boom tip displacement with stabilizer: (a) horizontal, (b) vertical

loaded cases with stabilizers are represented in Figs. 7(a) and 7(b), respectively. As in the previous cases without stabilizer the vertical displacement is shown to be much larger than the horizontal

Table 2 Peak dynamic displacements at the boom tip of the flexible crane system

Cases	Peak dynamic displacement (m)	
	Horizontal	Vertical
Empty	2.913	4.683
Full loaded	2.114	3.632
Full with CW	1.956	3.393
Full with fenders	1.192	2.046
Full with CW and fenders	1.058	1.823

Table 3 Differences in peak dynamic displacements at the boom tip between flexible and rigid crane systems

Cases	Flexible crane – rigid crane (m)	
	Horizontal	Vertical
Empty	0.255 (8.75%)	0.506 (10.81%)
Full loaded	0.193 (9.13%)	0.434 (11.95%)
Full with CW	0.181 (9.25%)	0.352 (10.37%)
Full with fenders	0.169 (14.18%)	0.259 (12.66%)
Full with CW and fenders	0.199 (18.81%)	0.218 (11.96%)

(*) relative difference to the peak dynamic displacement

displacement in all three cases. From Figs. 5~7 and Table 2, it is observed that the suppression of the dynamic displacement by counter weight is not remarkable, but the use of rubber fenders significantly suppresses the dynamic displacement at the boom tip. From the detailed numerical values given in Table 2, the relative reductions of the peak dynamic displacements with respect to the full loaded case with stabilizers are as follows: 6.58(7.47)% by counter weight, 43.67(43.61)% by rubber fender and 49.81(49.95)% by the combined use of counter weight and rubber fender, respectively. Here, the values in parenthesis indicate the relative reductions in the peak horizontal dynamic displacements. Meanwhile, as given in Table 3, the effect of the crane flexibility does not produce the remarkable change when compared with the cases without stabilizers, except for the horizontal dynamic displacements of the full loaded cases with rubber fenders. Referring to Fig. 3, it is because the insertion of rubber fenders between the mobile harbor and the container carrier makes the lateral deformation of the crane vertical columns larger, so that the resulting horizontal displacement at the boom tip becomes larger when the structural flexibility is considered.

5. Conclusions

A two-step sequential analytical-numerical technique has been introduced in this paper to solve the flexible dynamic response of RORI crane system installed within mobile harbor subject to the sinusoidal rolling excitation of wave at sea state 3. The concept underlined for this numerical technique is the fact that the total structural displacement is decomposed into the rigid motion and the relative flexible deformation. The rigid roll motion of mobile harbor was solved analytically, based upon the uncoupled linear roll wave theory, in which the natural frequency of the rigid

mobile harbor was obtained by the finite element analysis. Next, the structural dynamic response of the flexible RORI crane of mobile harbor was solved by transient finite element analysis, by applying the rigid roll motion solved analytically to the mass center of the mobile harbor as an external excitation. The hydrodynamic interaction between the mobile harbor and the sea wave was reflected by means of the added moment of inertia.

The effects of the crane flexibility and the stabilizers on the structural dynamic displacement at the boom tip were examined through the numerical experiments. The mobile harbor without stabilizer exhibits the rigid roll motion with the peak rolling angle 0.0783 rad at empty and 0.0589 rad at full, and the case considering the structure flexibility produces the peak dynamic tip displacements larger near by 10% than the rigid case. The suppression of the dynamic response at the boom tip by counter weight was not considerable such that the relative decrease in the peak dynamic displacement is less than 8%. But, the inflated rubber fender and the combined use of counter weight and inflated rubber fender show the significant dynamic suppression effect such that the relative decrease in the peak dynamic displacement is over 43% by fender and near 50% by the combined use of fender and counter weight. This suppression effect by the dynamic stabilizers is also confirmed through the comparison of the peak rigid roll angles of mobile harbor. It is convinced, through the current study, that the dynamic stability of both mobile harbor and RORI crane system could be successfully improved by appropriately combining dynamic dampers and counter weights.

However, wind load, random wave excitation, thrust and aerodynamic damping from the crane system were not included in the current study. So, the extension of the current study considering these additional effects deserves further work for more accurate structural dynamic analysis of the crane system for mobile harbor.

Acknowledgements

The financial support (2009. 7~2009. 12) for this work by the Mobile Harbor Research Center at Korea Advanced Institute of Science and Technology is gratefully acknowledged. This work was also supported by the Human Resources Development of the Korea Institute of Energy Technology Evaluation and Planning (KETEP) grant funded by the Korea Ministry of Knowledge Economy (No. 20113020020010).

References

- Biran, A.B. (2003), *Ship Hydrostatics and Stability*, Butterworth-Heinemann, Singapore.
- Cho, J.R. and Song, J.M. (2001), "Assessment of classical numerical models for the separate fluid-structure modal analysis", *J. Sound Vib.*, **239**(5), 995-1012.
- Cho, J.R., Song, J.M. and Lee, J.K. (2001), "Finite element techniques for the free-vibration and seismic analysis of liquid-storage tanks", *Finite Elem. Analy. D.*, **37**, 467-483.
- Godeauy, E. and Grist, J. (2006), *Bubble Benefits*, Technical Report, Siemens Water Technologies, USA.
- Lee, S.G. (2003), *Ship Motion and Maneuverability*, Pusan National University Press, Busan. (in Korean)
- Lim, O.K., Cho, J.R., Choi, E.H., Han, K.C. and Hwang, S.W. (2010), "Structural optimization and weight reduction analysis for type MH-A1", *Technical Report of Korean Ministry of Education, Science and Technology*, Seoul, Korea.

- Pierson, W.J. and Moskowitz, L. (1964), "A proposed spectral form for fully developed wind seas based on the similarity theory of S.A. Kitaigorodskii", *J. Geophys. Res.*, **69**(24), 5181-5203.
- Rajasankar, J., Iyer, N.R. and Apparao, T.V.S.R. (1993), "A new finite element model to evaluate added mass and for analysis of fluid-structure interaction problems", *Int. J. Numer. Meth. Eng.*, **36**, 997-1012.
- Senjanovic, I., Parunov, J. and Cipric, G. (1997), "Safety analysis of ship rolling in rough sea", *Chaos Soliton. Fractal.*, **8**(4), 659-680.